

ACCEPTED VERSION

Shaghayegh Dezvarei, Hiroki Onoda, Osami Shoji, Yoshihito Watanabe, Stephen G. Bell
Efficient hydroxylation of cycloalkanes by co-addition of decoy molecules to variants of the cytochrome P450 CYP102A1

Journal of Inorganic Biochemistry, 2018; 183:137-145

© 2018 Elsevier Inc. All rights reserved.

This manuscript version is made available under the CC-BY-NC-ND 4.0 license

<http://creativecommons.org/licenses/by-nc-nd/4.0/>

Final publication at <http://dx.doi.org/10.1016/j.jinorgbio.2018.03.001>

PERMISSIONS

<https://www.elsevier.com/about/our-business/policies/sharing>

Accepted Manuscript

Authors can share their accepted manuscript:

[24 months embargo]

After the embargo period

- via non-commercial hosting platforms such as their institutional repository
- via commercial sites with which Elsevier has an agreement

In all cases accepted manuscripts should:

- link to the formal publication via its DOI
- bear a CC-BY-NC-ND license – this is easy to do
- if aggregated with other manuscripts, for example in a repository or other site, be shared in alignment with our [hosting policy](#)
- not be added to or enhanced in any way to appear more like, or to substitute for, the published journal article

19 June 2020

<http://hdl.handle.net/2440/113527>

**Efficient hydroxylation of cycloalkanes by co-addition of decoy molecules to variants of the
cytochrome P450 CYP102A1**

Shaghayegh Dezvarei,^a Osami Shoji,^b Yoshihito Watanabe,^b and Stephen G. Bell^{a,*}

^a *Department of Chemistry, University of Adelaide, Adelaide, 5005, Australia*

^b *Department of Chemistry, Graduate School of Science, Nagoya University, Furo-cho, Chikusa-ku,
Nagoya, 464-8602, Japan*

Dr Stephen G. Bell

Phone: +61 8 8313 4822

E-mail: stephen.bell@adelaide.edu.au

Abstract

The wild type cytochrome P450 monooxygenase enzyme CYP102A1 (P450Bm3) has low activity for cycloalkane oxidation. The oxidation of these substrates by variants of this enzyme in combination with a selection of perfluorinated decoy molecules (PFCs) was investigated to improve productivity. The use of rate accelerating variants, which have mutations located outside of the substrate binding pocket as well as an active site variant of CYP102A1 (A74G/F87V/L188Q) all enhanced cycloalkane oxidation (C5 to C10). The addition of the decoy molecules to the WT and the rate accelerating mutants of CYP102A1 boosted the substrate oxidation rates even further. However, the levels of cycloalkanol product decreased with the larger alkanes when the decoy molecules were used with the mutant A74G/F87V/L188Q, which contained mutations within the substrate binding pocket. For the majority of the enzymes and PFC decoy molecule combinations the highest levels of oxidation were obtained with cyclooctane. When larger second generation decoy molecules, based on modified amino acids were utilised there was a significant improvement in the oxidation of the smaller cycloalkanes by the WT enzyme another variant. This resulted in significant improvements in biocatalytic oxidation of cyclopentane and cyclohexane. However, the use of these optimised decoy molecules did not significantly improve cycloalkane oxidation over the fluorinated fatty acid derivatives when combined with the best rate accelerating variant, R47L/Y51F/I401P. Overall our approach enabled the cycloalkanes to be oxidised 300- to 8000-fold more efficiently than the WT enzyme at product formation rates in excess of 500 and up to 1700 nmol.nmol-CYP⁻¹.min⁻¹.

Keywords: Monooxygenase; Cytochrome P450; Cycloalkanes; Hydroxylation; Heme proteins

1. Introduction

Cyclic alcohols are important building blocks for the production of valuable industrial chemicals such as cyclohexanol which is used in the production of Nylon-6,6 [1, 2]. The direct oxidation of cycloalkanes as a primary step for preparing the corresponding alcohols is therefore of significant interest [1]. The high stability of saturated C-H bonds in alkanes makes these compounds unreactive and they require forcing conditions such as high temperature and pressure, or a reactive oxidant in order to proceed [3, 4]. Various organic and inorganic methods have been used to facilitate the oxidation of cycloalkanes [5-7]; nevertheless these reactions remain challenging. The catalysts used in these chemical methods can be expensive, cannot be recovered or reused or proceed with low selectivity and the reactions often undergo further undesired oxidation. In addition these catalysts are often toxic and have an adverse impact on the environment [8].

Enzymatic approaches for C-H hydroxylation have emerged as an alternative method for alkane and cycloalkane oxidation [8-13]. Efficient enzyme biocatalysis for these processes would benefit industry and the environment as they occur under mild conditions in aqueous media. Taking advantage of enzymes as biocatalysts could overcome many of the hurdles of chemocatalysts, namely the expense, poor selectivity and environmental toxicity [13, 14]. The cytochrome P450 heme monooxygenases, are often Nature's enzyme of choice when selective oxidation of a complex substrate is required. They catalyse the hydroxylation of unreactive C-H bonds at ambient temperature and pressure using a reactive compound I iron-oxo species [15-24].

The CYP102A1 enzyme (P450Bm3) has often been employed as a biocatalyst to catalyse hydroxylation reactions [25-29]. This enzyme was discovered in the 1970s by Fulco, it was the third enzyme isolated from *Bacillus megaterium* and as such was named Bm3 [30, 31]. CYP102A1 is one of the most utilised P450 enzyme systems due to its high activity, solubility and self-sufficient nature. The electron transferring reductase domain is fused to the haem domain and it only needs the cofactor nicotinamide adenine dinucleotide phosphate (NADPH) and dioxygen to function [29].

Fatty acids of carbon chain length 12-15 are good substrates for this enzyme and hydroxylation of the acids occurred at subterminal position ($\omega-1$ to $\omega-3$) [29, 31]. Cycloalkanes are not the natural substrates of CYP102A1 therefore the enzyme must be modified to find conditions under which their hydroxylation will occur. Enzyme engineering by altering the amino acid sequences has been used to exploit this enzyme for alkane oxidation [25-27]. Two broad approaches have been utilised to adapt CYP102A1. The first makes changes in the substrate binding pocket (rational mutagenesis) [29, 32, 33] and the second involves directed evolution or random mutagenesis with a suitable screening method [28, 34-36].

Another approach which has been applied to enhance CYP102A1 biocatalysis is the use of decoy molecules [37]. Decoy molecules are inert dummy substrates which promote the catalytic activity of the enzyme [38]. Perfluorocarboxylic acids (PFCs) have been used with CYP102A1 with promising results for small alkanes and benzene [39]. The binding of the PFCs, which resemble the natural fatty acid substrates, initiates conformational changes in the heme domain enhancing substrate hydroxylation. The PFCs leave enough space in the substrate binding pocket for an additional molecule to bind. The decoys also appear to compel the substrates to bind more closely to the heme centre and facilitate the exclusion of water molecules. This is reflected in a lower proportion of the reducing equivalents being channelled into uncoupling pathways and resulted in higher levels of hydroxylation [39]. The use of decoy molecules can be combined with mutated variants to oxidise unnatural substrates with high catalytic productivity [39-41]. Second generation decoy molecules based on PFC modified L-amino acids have recently been synthesised to further enhance the activity of small molecules, such as propane. These bind to CYP102A1 with higher affinity than the PFCs. A crystal structure of the N-perfluorododecanoyl-L-tryptophan bound CYP102A1 heme domain has been obtained which revealed the conformational changes that are induced within the enzyme (Fig. 1).[42]

Here we use decoy molecules in combination with the wild-type (WT) enzyme and four engineered variants of CYP102A1 for the hydroxylation of differently sized cycloalkanes. Three of the variants employed KT2 (A191T/N239H/I259V/A276T/L353I), R19 (R47L/Y51F/H171L/Q307H/N319Y) and RP (R47L/Y51F/I401P) are rate accelerating forms of the enzyme, generated by random or rational mutagenesis or a combination of both [43, 44]. These have higher activity with non-natural substrates but maintain the selectivity of the WT enzyme [39-41]. For example the arginine 47 and tyrosine 51 residues, which have been altered in the R19 and RP variants, form hydrophilic interactions with fatty acid substrates and the changes render the active site more hydrophobic [28]. This would be expected to favour the oxidation of cycloalkanes but could reduce the effectiveness of the acid derived decoy molecules [28, 43]. The fourth variant GVQ (A74G/F87V/L188Q) was obtained from site saturation mutagenesis of three residues located in the active site or substrate access channel of CYP102A1 [25, 45, 46]. This variant increased the activity of the enzyme for hydrophobic substrates but can change the selectivity of oxidation as the modifications are in the active site of the enzyme [25, 47]. By using both first and second generation decoy molecules with different cycloalkanes we set out to gain a better understanding of the relationship between the size and shape of the decoy molecule and substrate to the performance of the enzyme catalysed oxidations.

2. Experimental

2.1 General

General reagents, organics and the PFC decoy molecules were obtained from Sigma-Aldrich, TCI, Fluorochem, Acros or VWR. The second generation decoy molecules, derived from amino acids were synthesised as described previously [42]. Buffer components, and isopropyl- β -D-thiogalactopyranoside (IPTG) were from Astral Scientific (Australia). UV/Vis spectroscopy was performed on an Agilent Cary 60 spectrophotometer. Gas chromatography was carried out on a Shimadzu Tracera GC coupled to Barrier discharge Ionization Detector (BID) detector using a Supelcowax column (30 m \times 0.32 mm \times 0.25 μ m) and helium as the carrier gas. For cyclopentane and cyclohexane the oven temperature was held at 60 °C for 3 min then increased at 5 °C min⁻¹ to 120 °C and maintained for 2 min then increased at 25 °C min⁻¹ to 220 °C. For cyclooctane and cyclodecane the oven temperature began at 100 °C for 3 min then increased at 8 °C min⁻¹ to 220 °C and held at this temperature for a further 2 min. The injector and detector temperature were 250 °C and 270 °C respectively. Gas Chromatography-Mass Spectrometry (GC-MS) data were collected on a Shimadzu GC-2010 coupled to a GC-MS-QP2010S detector. Both were equipped with a DB-5 MS fused silica column (30 m \times 0.25 mm, 0.25 μ m). The injector and interface were maintained at a constant temperature of 250 °C and 280 °C. The oven temperature was held at 60 °C for 1 min and then increased at 10 °C min⁻¹ up to 200 °C and it was maintained for 5 minutes. The product GC-MS/GC retention times were as follows: cyclopentanol, 1.8/5.7 min; cyclohexanol 3.3/7.8 min; cyclooctanol 7.3/8.3 min and cyclodecanol 10.9/10.8 min.

2.2 Protein expression and purification

Plasmids (pET28 and pET11d) containing the relevant gene were transformed into *E. coli* BL21(DE3) competent cells and grown on an LB plate containing the relevant antibiotic (Supplementary data) [28]. A single colony was used to inoculate 500 mL of 2xYT media containing trace elements solution (CaCl₂, ZnSO₄.7H₂O, MnSO₄.H₂O, Na₂-EDTA, FeCl₃.6H₂O,

CuSO₄·5H₂O, and CoCl₂·6H₂O) and grown at 37 °C and 110 rpm. The incubation temperature was lowered to 18 °C for 30 min before the addition of 0.02 % v/v benzyl alcohol and 2 % v/v ethanol. After a further 30 min, protein expression was induced by the addition of 0.1 mM IPTG and the growth was continued for 18 – 24 h. The cell pellet was then harvested by centrifugation (5000 g, 10 min, 4 °C) and resuspended in 40 mM phosphate buffer (pH 7.4, 1 mM DTT) and lysed by sonication on ice (30 cycles with 20 s on, 40 s off). Cell debris was removed by centrifugation (37000 g, 20 min, 4 °C) and the protein containing supernatant was loaded onto a DEAE Sepharose column (XK50, 200 mm × 40 mm; GE Healthcare) and eluted using a linear salt gradient of 80 – 400 mM (NH₄)₂SO₄ in phosphate buffer. The red-coloured fractions were combined and concentrated by centrifugation (1900 g, 4 °C) using ultrafiltration (30 kDa membrane, Vivacell 100, Sartorius). The protein was then desalted using a Sephadex G-25 medium grain column (250 mm × 40 mm; GE Healthcare). After desalting the protein was concentrated to approximately 10 ml by ultrafiltration and was loaded onto a Source-Q ion-exchange column (XK26, 80 mm × 30 mm; GE Healthcare) using an AKTA purifier (GE Healthcare) and eluted using a linear salt gradient of 16 × phosphate buffer (0 – 35 %). Fractions giving an A₄₁₉/A₂₈₀ > 0.5 were combined and concentrated by ultrafiltration. An equivalent volume of 80 % glycerol was added before the protein was filter-sterilised and stored at -20 °C.

2.3 Substrate turnover assays

NADPH turnover assays (final volume 1200 µL) were performed at 30 °C in Tris buffer (pH 7.4, 50 mM). The buffer was oxygenated before the addition of the other components, including 0.2 µM enzyme and 120 µg bovine liver catalase. Assays were sustained at 30 °C for 1 min prior to the addition of the decoy molecule (100 µM) and the substrate (1 mM) followed by NADPH (from a 20 mg mL⁻¹ stock, to a final concentration of ~320 µM; equivalent to 2 AU). A period of 10 s was allowed to elapse after cofactor addition before quantitating the NADPH oxidation rate by monitoring the decrease in the absorbance at 340 nm. The reactions were allowed to run until all the

reducing equivalents were consumed. The NADPH turnover rate was derived using $\epsilon_{340} = 6.22 \text{ mM}^{-1} \text{ cm}^{-1}$.

2.4 Extraction and GC analysis

Before extraction 200 μM of a *p*-cresol internal standard (10 μl of a 20 mM stock solution) was added, to 990 μL of the turnover. This mixture was then extracted with 400 μL ethyl acetate and the layers separated via centrifugation at 12000 *g* for 3 min. The extract was analysed by GC and a calibration curve was obtained in order to quantify the amount of product in each reaction. All the products were identified by coelution with authentic standards and MS analysis. The fatty acids turnovers were extracted, derivatised and analysed by GC-MS as described previously [48].

3. Results and Discussion

3.1 Cycloalkane oxidation by CYP102A1 variants

The heme domain in CYP102A1 is a funnel shaped shaft surrounded by hydrophobic residues e.g. Phe-42, Phe-87, Leu-181 and Leu-437 and is suited to the oxidation of medium to long chain fatty acids (Fig. 1). The WT enzyme was able to oxidise all the tested cycloalkane substrates, cyclopentane through to cyclodecane (Fig. 2 and Table 1). In all instances a single product arising from hydroxylation was observed (Scheme 1). However, the amount of product and the rate it was generated at was very low with the maximum activity observed for cyclooctane oxidation; 2.9 ± 0.7 nmol.nmol-CYP⁻¹.min⁻¹ (henceforth abbreviated to min⁻¹). All four of the CYP102A1 variants tested resulted in increased levels of oxidation product across the cycloalkanes. For all the cycloalkanes the RP variant resulted in the highest product formation rate. The trends in the remaining mutants did show variation depending on the substrate (Table 1). For example the GVQ variant, which should increase the size of the substrate binding pocket was an improved biocatalyst for cyclodecane oxidation compared to R19 and KT2 (Table 1). However, the R19 mutant was better at oxidising both cyclooctane and cyclohexane than GVQ (Table 1).

The size of the cycloalkane substrate had a significant effect on the rate of product formation. The highest turnover rate, up to 1050 min⁻¹, observed for all the variants, including GVQ, was with cyclooctane (Table 1). The maximum activity for both cyclohexane and cyclodecane being 411 and 283 min⁻¹, respectively. The product formation rate with the smallest substrate cyclopentane was significantly slower, with the highest product formation rate observed being 62 min⁻¹. Overall; by using a selection of CYP102A1 variants we were able to improve the product formation rates of cycloalkane oxidation from 160-fold for cyclodecane to 1500-fold for cyclohexane (Table 1). We also tested cyclododecane with our variants and decoy molecules but little or no oxidation metabolites were observed (data not shown). The R19 and RP variants, which contain the Arg47Leu and Tyr51Phe mutations, located at the entrance to the substrate access channel to allow easier access of hydrophobic substrates, were the most active variants (Table 1).

3.2 The effect of PFC decoy molecules on cycloalkane oxidation

Next we assessed if cycloalkane oxidation could be improved using PFC based decoy molecules (PFC8 to PFC10) [37, 39]. The addition of PFCs enhanced the productive turnover of the WT enzyme with all four cycloalkanes (Fig. 2 and Table 1). In agreement with previous results, the greatest increases in the product formation rate for all the substrates were observed with PFC9 and PFC10. It is of note that the catalytic turnover with PFC10 was substantially higher than that achieved when using PFC9 for the smaller cycloalkanes (Table 1). The results obtained with these two decoy molecules and the larger cyclooctane and cyclodecane substrates were comparable (Table 1). The overall product formation rates obtained for the WT enzyme combined with these first generation decoy molecules was lower than with the mutant forms of CYP102A1, e.g. 204 min^{-1} for cyclooctane oxidation by the WF/PFC10 combination versus 1050 min^{-1} for the RP variant alone (Table 1).

The addition of these fatty acid based PFC decoy molecules also upgraded cycloalkane oxidation with the KT2, R19 and the RP variants. With the R19 and RP variants the PFC10 decoy molecule also resulted in the highest turnover rates. The KT2/PFC9 combination was better than that with PFC10 for all the cycloalkanes (Fig. 3 and Table 1). This suggested that changes in the conformation or structure of the mutant enzymes may affect the decoy molecule/substrate preference and therefore the overall activity.

The addition of the decoy molecules resulted in differing levels of enhancement with each CYP102A1 mutant compared to oxidation activity of the variant itself. In all instances the magnitude of the upturn in the product formation rates was lower than those observed with the WT enzyme (Table 1). Across all substrates the improvement observed with KT2 was greater than that of the R19 and RP variants. The latter two CYP102A1 mutants contain the RLYF double mutation at the entrance to the substrate access channel and also have higher innate product formation activities with the cycloalkanes. Despite the lower relative levels of enhancement compared to WT

and KT2, the combination of the decoy molecules with the R19 or RP variants resulted in the highest oxidation rates (Fig. 3 and Table 1). The R19/PFC10 combination generated the maximum rate of hydroxylation with cyclodecane and cyclohexane while the addition of PFC10 to the RP variant generated the highest activities with cyclopentane and cyclooctane (Fig. 3 and Table 1).

As with the WT enzyme the majority of the CYP102A1 variant and decoy molecule combinations hydroxylated cyclooctane more effectively than the other cycloalkanes. Cyclopentane or cyclodecane oxidation occurred with the lowest efficiency depending on the combination used. The exception was the KT2 variant, which when coupled with certain decoy molecules, catalysed cyclohexane oxidation more rapidly than cyclooctane under the assay conditions (Table 1). Cyclopentane oxidation peaked at 200 min^{-1} , a greater than 3000-fold improvement over the WT enzyme. Cyclohexane oxidation with the R19 and PFC10 decoy molecule occurred at a rate of 938 min^{-1} . The improvements achieved with cyclodecane and cyclooctane were more modest being, 300-fold for (524 min^{-1}) and 560-fold (1700 min^{-1}), respectively. Importantly, for the best CYP102A1 variant/decoy molecule combinations the coupling efficiency, which is a measure of the productive use of the NADPH cofactor, was high e.g. 81 % for cyclooctane and RP/PFC10. The concerted effect of the CYP102A1 variants and decoy molecules resulted in a greater degree of enhancement with the smaller substrates which resulted in the product formation rate of cyclohexane (>3000-fold improvement) surpassing that of cyclodecane in their best turnovers (Table 1).

3.3 The effect of PFC decoy molecules on cycloalkane oxidation by the GVQ variant

The effect of the decoy molecules with the GVQ mutant differed from those observed with the other variants. The addition of all three decoy molecules resulted in a modest enhancement of cyclopentane oxidation, with the GVQ/PFC9 combination resulting in the highest product formation rate ($59 \pm 3.3 \text{ min}^{-1}$, Table 1). Only PFC8 and PFC9 improved the catalytic performance of cyclohexane oxidation but in these instance the coupling efficiency of the turnover decreased

(Table 1). The decoy molecules diminished the amount of product generated with cyclooctane (Fig. 3 and Fig. S1) and cyclodecane. With these larger substrates the shorter PFC8 decoy molecule had less of a detrimental effect on the levels of product formation (Table 1).

The GVQ variant is the only form of CYP102A1 tested in this work which has mutations in the substrate binding pocket/access channel of the enzyme close to the heme. This could have a significant effect on how the fatty acid based decoy molecules interact and therefore bind to the enzyme. The Phe87 residue has been shown to have a prominent role in substrate binding in CYP102A1 [28, 46, 49, 50]. To assess if the GVQ variant alters the binding of the fatty acid molecules we investigated the oxidation of decanoic, dodecanoic and tetradecanoic acids. The GVQ variant altered the product distribution of dodecanoic and tetradecanoic acids compared to the WT enzyme (Table 1 and Fig. S2). In the GVQ variant the hydroxylation was shifted away from the ω -terminus which suggested that the fatty acids were bound differently compared to the WT enzyme and that a greater proportion of the subterminal carbons of the fatty acid chain were located over the heme iron. This mutant was also able to oxidise decanoic acid whereas the WT enzyme was only capable of generating a trace amount of the hydroxylated metabolites (Table 1 and Fig. S2).

These results confirm that the GVQ variant binds fatty acid like molecules in a different manner than the WT enzyme. Therefore one plausible explanation for the different effect of the decoy molecules with the GVQ variant is that the altered PFC binding orientation results in the decoy molecules, which contain strong unreactive C-F bonds, being positioned in between the cycloalkane substrate and the heme. While this enabled turnover of the P450 catalytic cycle it reduced productive cycloalkanol formation (Table S1). In an effort to assess if other decoy molecules could improve the productivity of the GVQ mutant we examined the oxidation of cyclooctane with PFC3 through to PFC7 as well as 4-fluoro- and pentafluorobenzoic acid (Fig. 4). None of these molecules stimulated the NADPH oxidation rate or the level of product formation above that of the GVQ variant alone (Table S1).

3.4 The effect of second generation decoy molecules on cycloalkane oxidation

It is worth noting that PFC8 to PFC10 have been shown to be the optimal fatty acid derived decoy molecules and that shorter and longer versions, such as PFC11, reduce the activity of oxidation [37]. In an effort to explore how the structure of the coadditive effects the cycloalkane hydroxylation in more detail we utilised second generation decoy molecules which are based on PFCs modified with L-amino acids, PFC9-L-Ala, PFC9-L-Leu and PFC9-L-Phe (Fig. 4) [42]. The use of these decoys allowed CYP102A1 to catalytically hydroxylate the small gaseous alkanes ethane and propane [42]. When combined with the WT enzyme these second generation molecules also enhanced the rate of NADPH oxidation in the cycloalkane turnovers above those obtained with the first generation PFC decoy molecules. (Table S2). The improvements in the coupling efficiency and the product formation rate with the larger C8 and C10 cycloalkanes were modest (Table S2). However, a marked upturn in the coupling efficiency, and therefore the overall product formation rate, was observed with cyclopentane and cyclohexane (Fig. 5). The rate of product formation when the PFC9-L-Phe decoy molecule was added the WT enzyme was the greatest for both of these cycloalkanes (Fig. 5 and Table S2), resulting in a 21-fold improvement over the PFC10 decoy molecule with cyclopentane (PFR $949 \pm 35 \text{ min}^{-1}$) and a 5-fold enhancement with cyclohexane (PFR $725 \pm 46 \text{ min}^{-1}$).

The second generation decoy molecules were also combined with the RP and KT2 variants to assess if they could enhance cycloalkane oxidation. The results were mixed with cyclohexane the RP/PFC9-L-Ala couple was marginally better than the R19/PFC10 combination (1010 ± 13 versus $938 \pm 20 \text{ min}^{-1}$, Fig. 5, Table 1 and S2). The hydroxylation of cyclopentane with RP was also improved using the second generation decoys over the best fluorinated fatty acid derived molecules (845 ± 21 versus $501 \pm 33 \text{ min}^{-1}$, Table 1 and S2). Due to lower coupling efficiency, the product formation rate with RP/PFC9-L-Ala ($845 \pm 21 \text{ min}^{-1}$) was lower than achieved with the WT/PFC9-L-Phe combination (Fig. 5 and Table S2). With the RP variant and the cyclooctane and cyclodecane

substrates all the turnovers with the second generation decoys showed lower product formation than PFC10, with PFC9-L-Ala being the best. The difference between the productivity of the RP variant for cyclooctane and cyclodecane when partnered with the second generation decoy molecules compared to the smaller cycloalkanes is perhaps due to the bulkier nature of the decoy which may hamper access of the larger substrate in the narrow access channel of the enzyme (Fig. 1, Fig. S3 and Table S2). The crystal structure of the heme domain of CYP102A1 with the second generation decoy molecule PFC9-L-Trp bound revealed that Tyr51 formed a hydrogen bond with the amide carbonyl group of the decoy (Fig. 1). In the RP variant Tyr51 has been mutated to a phenylalanine and as a result the decoy molecule may bind in a different way. Overall, PFC9-L-Ala was the best decoy molecule for all the cycloalkanes with RP in contrast to the WT enzyme which was better with PFC9-L-Phe or PFC9-L-Leu.

When the second generation decoy molecules were used with the KT2 variant the product formation rate for the oxidation of the smaller cycloalkanes increased dramatically. This was predominantly due to superior turnover the catalytic cycle, as measured by the NADPH oxidation rate. The upturn for the larger substrates was not as significant. As with the WT enzyme the PFC9-L-Phe combined with KT2 give rise to the highest product formation rates for smaller cycloalkanes with PFC9-L-Leu being better with the larger. The formation rate of cyclopentanol and cyclohexanol with PFC9-L-Phe partnered with KT2 were the highest observed in this study, with the smaller substrates, and were $1330 \pm 68 \text{ min}^{-1}$ and $1430 \pm 76 \text{ min}^{-1}$, respectively (Fig. 5 and Table S2). The combination of the second generation decoy molecules with GVQ variant also diminished the oxidation activity of the enzyme. (Table S1)

Overall our results show that combining decoy molecules and CYP102A1 variant resulted in increased rates and efficiency of cycloalkane oxidation. The rate accelerating variants and the decoy molecules are both hypothesised to, and have been shown by crystal structure analysis to, enable the enzyme to more readily access catalytically ready conformations resulting in increased productivity.

They also appear to facilitate a favourable binding position for the cycloalkane substrate in relation to the heme which often resulted in an elevated coupling efficiency. The second generation decoy molecules seem to induce a greater effect on the WT and KT2 enzymes which resulted in more frequent turnover of the catalytic cycle. However with the RP variant these decoys were often not as effective as the PFC molecules or as they were with the WT and KT2 enzymes. Second generation decoy molecules of different size were more effective with the KT2 and WT enzymes compared to the RP and GVQ variants suggesting that they interact differently across the mutant forms of CYP102A1.

4. Conclusion

Cycloalkanes bear little resemblance to the fatty acid based natural substrates of CYP102A1 but the activity of CYP102A1 towards these unnatural substrates was enhanced by utilising rate accelerating variants and decoy molecules. The best variants contained the R47L/Y51F mutations at the entrance of substrate access channel (R19 and RP). Their combination with the first generation PFC10 decoy molecule provided high rates of hydroxylation. The addition of the decoy molecules to the R19 and RP variants had less of an impact compared to the innate product formation rate but still resulted in a significant enhancement in monooxygenase activity. The larger second generation decoy molecule PFC9-Phe boosted the productivity of the cyclopentane and cyclohexane turnovers of the WT enzyme and KT2 variant even further when compared to PFC10. The GVQ variant showed contradictory results and addition of decoy molecules reduced the level of product formation. This is most likely due to a different binding orientation of the PFC decoy molecule which hampers hydroxylation. That the highest productivity with larger substrates, such as cyclooctane and cyclodecane, could be achieved with the first generation decoys suggests that the CYP102A1 variants can accept molecules of moderate size in conjunction with the PFC molecules. The larger second generation decoy molecules enhanced biocatalysis with the smaller substrates to a significantly greater degree inferring that the active site is more restricted when these are bound to the enzyme. The combination of CYP102A1 variants and decoy molecules boosted the efficiency of cycloalkane oxidation by up to 8000-fold for the substrates tested here.

Acknowledgements

S.G.B. acknowledges the ARC for a Future Fellowship (FT140100355). The authors also acknowledge the University of Adelaide International Postgraduate Award (for S.D.) and for a Priority Partner Grant (University of Nagoya). The authors thank Prof. Luet-Lok Wong (University of Oxford, UK) for the gene constructs of the CYP101A1 and CYP102A1 variants.

References

- [1] U. Schuchardt, D. Cardoso, R. Sercheli, R. Pereira, R.S. da Cruz, M.C. Guerreiro, D. Mandelli, E.V. Spinacé, E.L. Pires, *Appl. Catal. A*, 211, (2001), 1-17.
- [2] R. Jevtic, P.A. Ramachandran, M.P. Dudukovic, *Chem. Eng. Res. Des.*, 88, (2010), 255-262.
- [3] R.H. Crabtree, *Dalton Trans.*, (2001), 2437-2450.
- [4] T. Newhouse, P.S. Baran, *Angew. Chem. Int. Ed. Engl.*, 50, (2011), 3362-3374.
- [5] A.E. Shilov, G.B. Shul'pin, *Chem. Rev.*, 97, (1997), 2879-2932.
- [6] N.M.F. Carvalho, A. Horn Jr, O.A.C. Antunes, *Appl. Catal.*, A, 305, (2006), 140-145.
- [7] M.D. Godbole, M.P. Puig, S. Tanase, H. Kooijman, A.L. Spek, E. Bouwman, *Inorg. Chim. Acta*, 360, (2007), 1954-1960.
- [8] F. Hollmann, I.W.C.E. Arends, K. Buehler, A. Schallmeyer, B. Bühler, *Green Chem.*, 13, (2011), 226-265.
- [9] S.C. Maurer, K. Kühnel, L.A. Kaysser, S. Eiben, R.D. Schmid, V.B. Urlacher, *Adv. Synth. Catal.*, 347, (2005), 1090-1098.
- [10] E. Weber, A. Seifert, M. Antonovici, C. Geinitz, J. Pleiss, V.B. Urlacher, *Chem. Commun.*, 47, (2011), 944-946.
- [11] A. Narayan, R. H., G. Jiménez-Osés, P. Liu, S. Negretti, W. Zhao, M.M. Gilbert, R.O. Ramabhadran, Y.-F. Yang, L.R. Furan, Z. Li, L.M. Podust, J. Montgomery, K.N. Houk, D.H. Sherman, *Nat. Chem.*, 7, (2015), 653-660.
- [12] F. Hollmann, *Catal. Lett.*, 143, (2013), 982-982.
- [13] A. Wells, H.-P. Meyer, vol. 6, Wiley-Blackwell, 2014, pp. 918-920.
- [14] W.-D. Woggon, *Acc. Chem. Res.*, 38, (2005), 127-136.
- [15] E.M. Isin, F.P. Guengerich, *Biochim. Biophys. Acta*, 1770, (2007), 314-329.
- [16] D. Mansuy, *Comp. Biochem. Physiol. C Pharmacol. Toxicol. Endocrinol.*, 121, (1998), 5-14.
- [17] C.-H. Yun, K.-H. Kim, D.-H. Kim, H.-C. Jung, J.-G. Pan, *Trends Biotechnol.*, 25, (2007), 289-298.
- [18] V.B. Urlacher, S. Eiben, *Trends Biotechnol.*, 24, (2006), 324-330.
- [19] F.P. Guengerich, *Nat. Rev. Drug Discov.*, 1, (2002), 359-366.
- [20] R. Bernhardt, *J. Biotechnol.*, 124, (2006), 128-145.
- [21] M. Sono, M.P. Roach, E.D. Coulter, J.H. Dawson, *Chem. Rev.*, 96, (1996), 2841-2888.
- [22] J. Rittle, M.T. Green, *Science*, 330, (2010), 933-937.
- [23] I.G. Denisov, T.M. Makris, S.G. Sligar, I. Schlichting, *Chem. Rev.*, 105, (2005), 2253-2277.
- [24] C.M. Krest, E.L. Onderko, T.H. Yosca, J.C. Calixto, R.F. Karp, J. Livada, J. Rittle, M.T. Green, *J. Biol. Chem.*, 288, (2013), 17074-17081.
- [25] D. Appel, S. Lutz-Wahl, P. Fischer, U. Schwaneberg, R.D. Schmid, *J. Biotechnol.*, 88, (2001), 167-171.
- [26] Edgardo T. Farinas, U. Schwaneberg, A. Glieder, Frances H. Arnold, *Adv. Synth. Catal.*, 343, (2001), 601-606.
- [27] A. Glieder, E.T. Farinas, F.H. Arnold, *Nature Biotechnol.*, 20, (2002), 1135-1139.
- [28] C.J. Whitehouse, S.G. Bell, H.G. Tufton, R.J. Kenny, L.C. Ogilvie, L.L. Wong, *Chem. Commun.*, (2008), 966-968.
- [29] C.J. Whitehouse, S.G. Bell, L.L. Wong, *Chem. Soc. Rev.*, 41, (2012), 1218-1260.
- [30] H. Schwalb, L. Owers Narhi, A.J. Fulco, *Biochim. Biophys. Acta Gen. Subj.*, 838, (1985), 302-311.
- [31] A.J. Fulco, *Annu. Rev. Pharmacol. Toxicol.*, 31, (1991), 177-203.
- [32] S.T. Jung, R. Lauchli, F.H. Arnold, *Curr. Opin. Biotechnol.*, 22, (2011), 809-817.
- [33] J.A. McIntosh, C.C. Farwell, F.H. Arnold, *Curr. Opin. Chem. Biol.*, 19, (2014), 126-134.
- [34] C.F. Oliver, S. Modi, M.J. Sutcliffe, W.U. Primrose, L.-Y. Lian, G.C.K. Roberts, *Biochemistry*, 36, (1997), 1567-1572.
- [35] J.B.Y.H. Behrendorff, W. Huang, E.M.J. Gillam, *Biochem. J.*, 467, (2015), 1-15.

- [36] M.W. Peters, P. Meinhold, A. Glieder, F.H. Arnold, *J. Am. Chem. Soc.*, 125, (2003), 13442-13450.
- [37] O. Shoji, T. Kunimatsu, N. Kawakami, Y. Watanabe, *Angew. Chem. Int. Ed. Engl.*, 52, (2013), 6606-6610.
- [38] O. Shoji, T. Fujishiro, H. Nakajima, M. Kim, S. Nagano, Y. Shiro, Y. Watanabe, *Angew. Chem. Int. Ed. Engl.*, 46, (2007), 3656-3659.
- [39] S.D. Munday, O. Shoji, Y. Watanabe, L.L. Wong, S.G. Bell, *Chem. Commun.*, 52, (2016), 1036-1039.
- [40] S.D. Munday, S. Dezvarei, S.G. Bell, *ChemCatChem*, 8, (2016), 2789-2796.
- [41] S.D. Munday, S. Dezvarei, I.C.K. Lau, S.G. Bell, *ChemCatChem*, 9, (2017), 2512-2522.
- [42] Z. Cong, O. Shoji, C. Kasai, N. Kawakami, H. Sugimoto, Y. Shiro, Y. Watanabe, *ACS Catal.*, 5, (2015), 150-156.
- [43] C.J. Whitehouse, S.G. Bell, W. Yang, J.A. Yorke, C.F. Blanford, A.J. Strong, E.J. Morse, M. Bartlam, Z. Rao, L.L. Wong, *Chembiochem*, 10, (2009), 1654-1656.
- [44] C.J. Whitehouse, W. Yang, J.A. Yorke, B.C. Rowlatt, A.J. Strong, C.F. Blanford, S.G. Bell, M. Bartlam, L.L. Wong, Z. Rao, *Chembiochem*, 11, (2010), 2549-2556.
- [45] H.M. Li, L.H. Mei, V.B. Urlacher, R.D. Schmid, *Appl. Biochem. Biotechnol.*, 144, (2008), 27-36.
- [46] Q.S. Li, U. Schwaneberg, P. Fischer, R.D. Schmid, *Chem. Eur. J.*, 6, (2000), 1531-1536.
- [47] C.-H. Chiang, R. Ramu, Y.-J. Tu, C.-L. Yang, K.Y. Ng, W.-I. Luo, C.H. Chen, Y.-Y. Lu, C.-L. Liu, S.S.F. Yu, *Chem. Eur. J.*, 19, (2013), 13680-13691.
- [48] S.D. Munday, N.K. Maddigan, R.J. Young, S.G. Bell, *Biochim. Biophys. Acta*, 1860, (2016), 1149-1162.
- [49] S. Graham-Lorence, G. Truan, J.A. Peterson, J.R. Falck, S. Wei, C. Helvig, J.H. Capdevila, *J. Biol. Chem.*, 272, (1997), 1127-1135.
- [50] M.A. Noble, C.S. Miles, S.K. Chapman, D.A. Lysek, A.C. MacKay, G.A. Reid, R.P. Hanzlik, A.W. Munro, *Biochem. J.*, 339 (Pt 2), (1999), 371-379.

Table 1 NADPH consumption and product formation rates of cycloalkane turnovers with WT CYP102A1 and the rate accelerating variants with and without the presence of the first generation of decoy molecules. Coupling efficiency which is the percentage of NADPH utilised for the formation of cycloalkanol products are also provided. NADPH oxidation rate (NADPH) and product formation rate (PFR) are reported as mean \pm S.D. ($n \geq 3$) and given in nmol(nmol-CYP)⁻¹min⁻¹. The optimal decoy molecule has been highlighted for each enzyme/cycloalkane combination in bold.

	cyclopentane			cyclohexane			cyclooctane			cyclodecane		
	NADPH	coupling	PFR	NADPH	coupling	PFR	NADPH	coupling	PFR	NADPH	coupling	PFR
WT	17 \pm 0.7	1 \pm 0	0.15 \pm 0	20 \pm 2	1 \pm 0	0.3 \pm 0.1	53 \pm 3	6 \pm 0	3 \pm 0.2	61 \pm 1	3 \pm 0	1.7 \pm 0.1
WT/8	77 \pm 1	2 \pm 0	1.76 \pm 0.1	94 \pm 3	35 \pm 2	33 \pm 2.4	145 \pm 17	63 \pm 5	91 \pm 4	83 \pm 1	25 \pm 0	20 \pm 1
WT/9	87 \pm 3	5 \pm 0	4 \pm 0.2	175 \pm 6	49 \pm 2	85 \pm 6	309 \pm 12	64 \pm 0	197 \pm 7	118 \pm 4	29 \pm 2	34 \pm 1
WT/10	257 \pm 2	13 \pm 0	45 \pm 1	443 \pm 10	33 \pm 3	144 \pm 10	438 \pm 23	47 \pm 4	204 \pm 18	249 \pm 10	15 \pm 1	37 \pm 2
R19	76 \pm 4	5 \pm 1	3 \pm 0.1	594 \pm 21	60 \pm 2	355 \pm 18	964 \pm 7	74 \pm 1	708 \pm 3	196 \pm 18	37 \pm 2	72 \pm 2
R19/8	133 \pm 6	7 \pm 1	9 \pm 0.9	741 \pm 34	56 \pm 1	416 \pm 24	1170 \pm 13	76 \pm 3	885 \pm 26	656 \pm 9	41 \pm 2	271 \pm 20
R19/9	205 \pm 4	15 \pm 0	32 \pm 1.5	854 \pm 43	58 \pm 0	402 \pm 22	1260 \pm 21	72 \pm 1	906 \pm 18	835 \pm 24	44 \pm 2	367 \pm 18
R19/10	575 \pm 7	25 \pm 2	142 \pm 9	1620 \pm 12	58 \pm 1	938 \pm 20	1700 \pm 13	75 \pm 1	1280 \pm 19	1180 \pm 5	44 \pm 1	524 \pm 9
RP	352 \pm 14	18 \pm 0	62 \pm 3	1210 \pm 24	34 \pm 1	411 \pm 2	1570 \pm 46	67 \pm 1	1050 \pm 16	807 \pm 11	35 \pm 2	283 \pm 16
RP/8	965 \pm 28	37 \pm 3	359 \pm 17	1490 \pm 6	42 \pm 2	631 \pm 26	2060 \pm 24	74 \pm 0	1530 \pm 15	932 \pm 18	38 \pm 2	357 \pm 26
RP/9	1140 \pm 43	42 \pm 2	481 \pm 40	1520 \pm 44	40 \pm 0	609 \pm 15	2030 \pm 17	75 \pm 0	1520 \pm 10	1100 \pm 14	39 \pm 1	423 \pm 14
RP/10	1180 \pm 40	42 \pm 1	501 \pm 33	1940 \pm 24	38 \pm 1	741 \pm 15	2100 \pm 32	81 \pm 2	1700 \pm 25	1200 \pm 26	38 \pm 3	451 \pm 42
KT2	131 \pm 8	17 \pm 0	23 \pm 2	244 \pm 4	29 \pm 1	70 \pm 2.7	231 \pm 6	45 \pm 2	104 \pm 1	116 \pm 1	27 \pm 1	31 \pm 1
KT2/8	341 \pm 10	34 \pm 0	117 \pm 8	912 \pm 36	52 \pm 2	478 \pm 27	909 \pm 14	57 \pm 2	518 \pm 18	595 \pm 21	39 \pm 1	233 \pm 1
KT2/9	901 \pm 16	44 \pm 3	426 \pm 27	1590 \pm 37	45 \pm 2	714 \pm 54	1160 \pm 20	54 \pm 2	627 \pm 24	1090 \pm 21	28 \pm 2	308 \pm 15
KT2/10	1340 \pm 29	34 \pm 0	397 \pm 4	1960 \pm 17	27 \pm 3	538 \pm 51	1450 \pm 12	33 \pm 0	473 \pm 4	1740 \pm 21	11 \pm 0	185 \pm 4
GVQ	100 \pm 4	4 \pm 0	3.3 \pm 0.1	323 \pm 28	25 \pm 2	81 \pm 9	660 \pm 22	51 \pm 0	324 \pm 4	1010 \pm 43	24 \pm 1	241 \pm 8
GVQ/8	862 \pm 15	5 \pm 1	40 \pm 1	855 \pm 21	19 \pm 1	166 \pm 14	988 \pm 24	32 \pm 2	319 \pm 19	1050 \pm 29	20 \pm 1	208 \pm 15
GVQ/9	1490 \pm 27	4 \pm 3	159 \pm 3	1980 \pm 52	9 \pm 0	183 \pm 7	1310 \pm 7	12 \pm 0	164 \pm 8	1180 \pm 59	9 \pm 0	110 \pm 4
GVQ/10	1530 \pm 54	2 \pm 1	27 \pm 1	1660 \pm 26	5 \pm 0	75 \pm 10	1760 \pm 24	6 \pm 1	110 \pm 11	1580 \pm 15	5 \pm 0	72 \pm 1

Table 2 Product distribution of fatty acids oxidation by CYP102A1 WT and GVQ variants. Very little product was formed with the WT and decanoic acid (Fig. S2).

Fatty acid	%Product	WT	GVQ
tetradecanoic acid	ω -1	48	7
	ω -2	25	16
	ω -3	24	31
	ω -4	1	16
	ω -5	0.5	25
	ω -6	1	5
dodecanoic acid	ω -1	37	26
	ω -2	28	37
	ω -3	35	34
	ω -4	0	1
	ω -5	0	2
decanoic acid	ω -1	-	55
	ω -2	-	22
	ω -3	-	23

Scheme 1. Production of cyclic alcohols by CYP102A1.

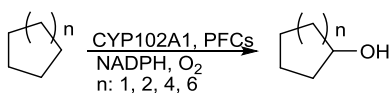


Figure 1 The crystal structure of CYP102A1 with PFC9-L-Trp decoy molecule (PDB: 3WSP), the access channel (grey wireframe) and hydrophobic or mutated residues (yellow) are shown. The hydrogen bond between PFC9-L-Trp/Y51 and PFC9-L-Trp/A74 (dashed line) and the distance between PFC9-L-Trp and heme domain (dashed line) have been indicated.

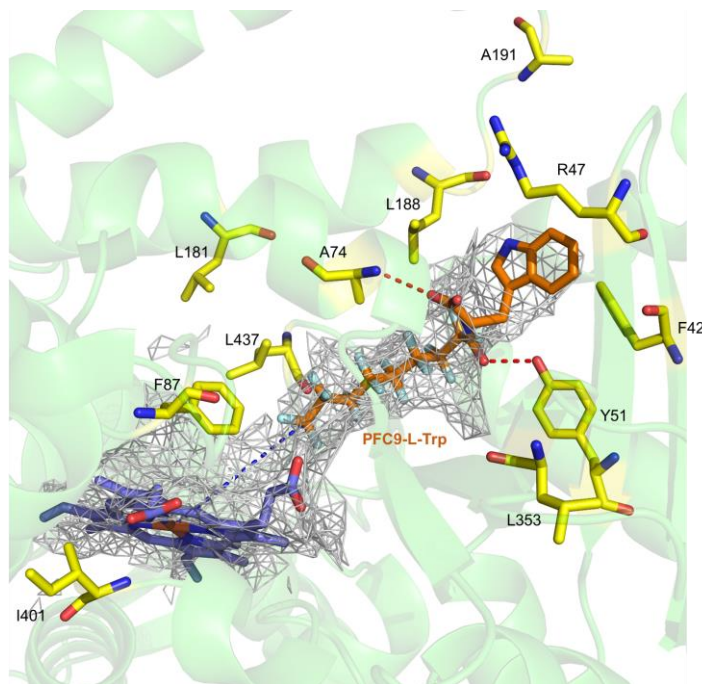


Figure 2 GC analysis of turnovers of cyclopentane, cyclohexane, cyclooctane and cyclodecane with WT (solid black), WT/PFC10 (grey dash) and the optimised variant/ PFC for each substrate. The optimal biocatalyst combination for cyclopentane and cyclooctane is RP/PFC10 (red) while R19/PFC10 (blue) generated more product with cyclohexane and cyclodecane (full data provided in Table 1).

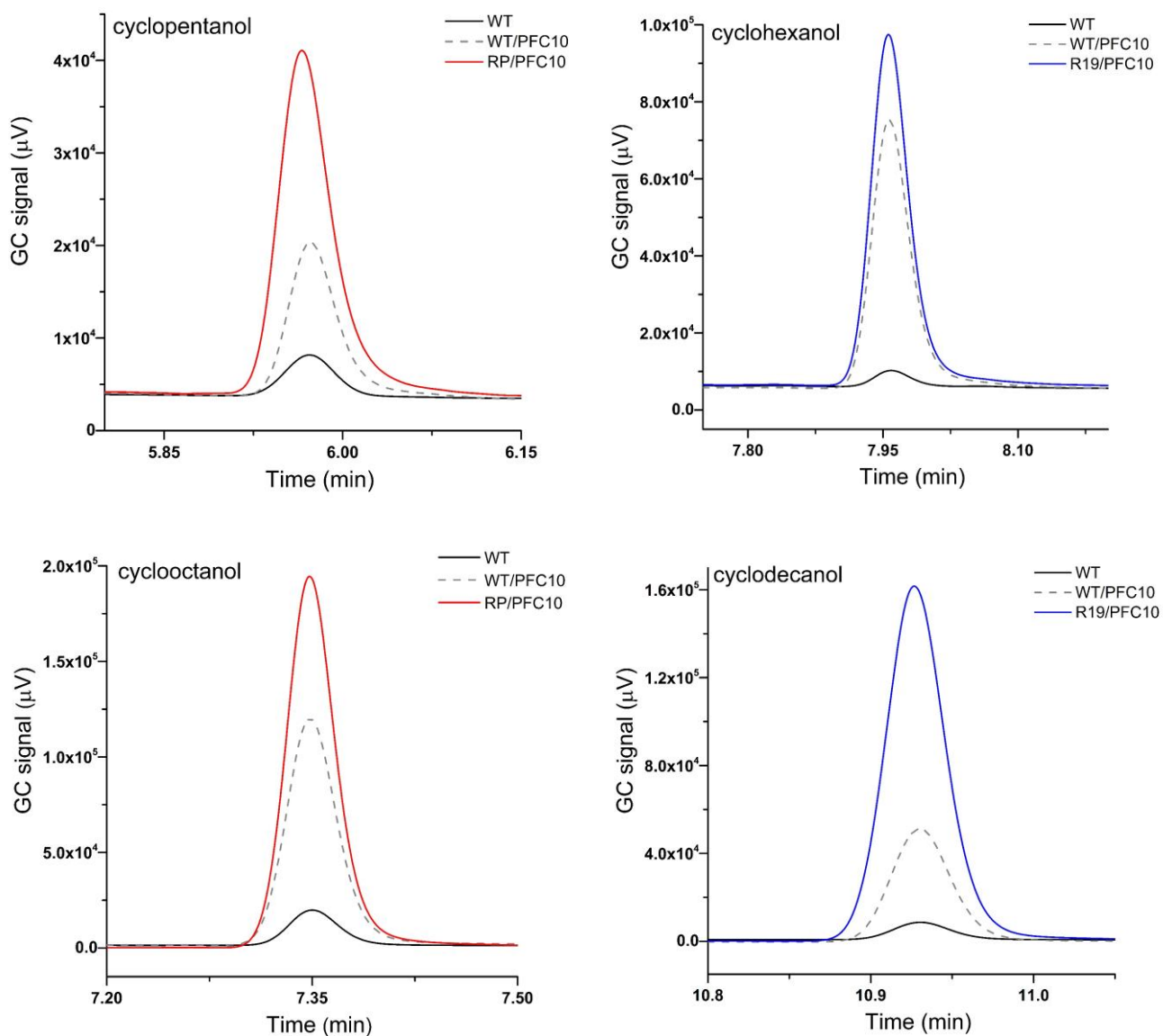


Figure 3 NADPH oxidation (grey) and product formation rates (blue-lined) of the optimal combination of the PFC decoy molecules with CYP102A1 WT and its variants for cyclopentane, cyclohexane, cyclooctane and cyclodecane hydroxylation. NADPH oxidation and product formation rates are reported as the mean ($n \geq 3$) and given in $\text{nmol}(\text{nmol-CYP})^{-1}\text{min}^{-1}$ (full data provided in Table 1).

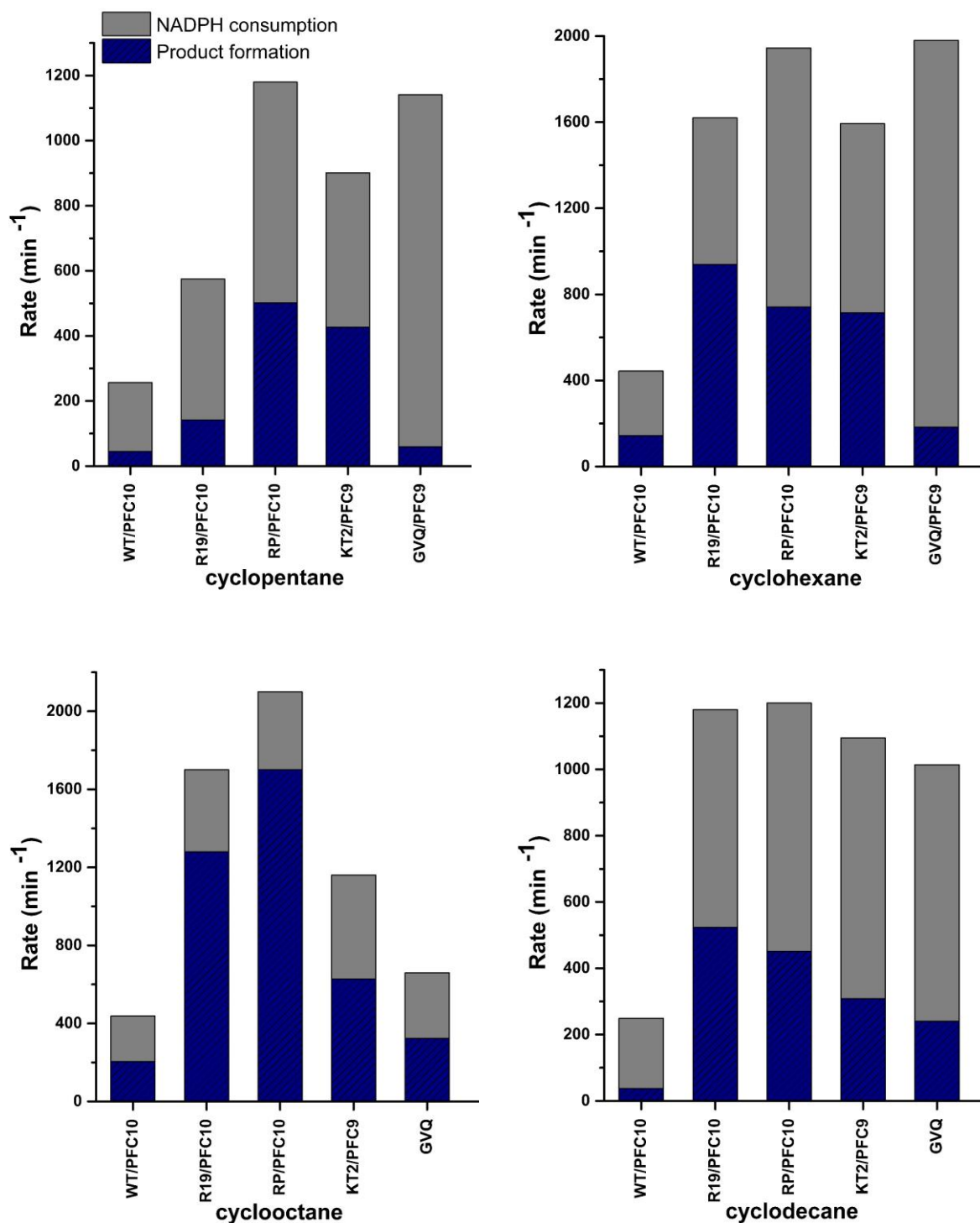


Figure 4 The structures of the decoy molecules used in this study.

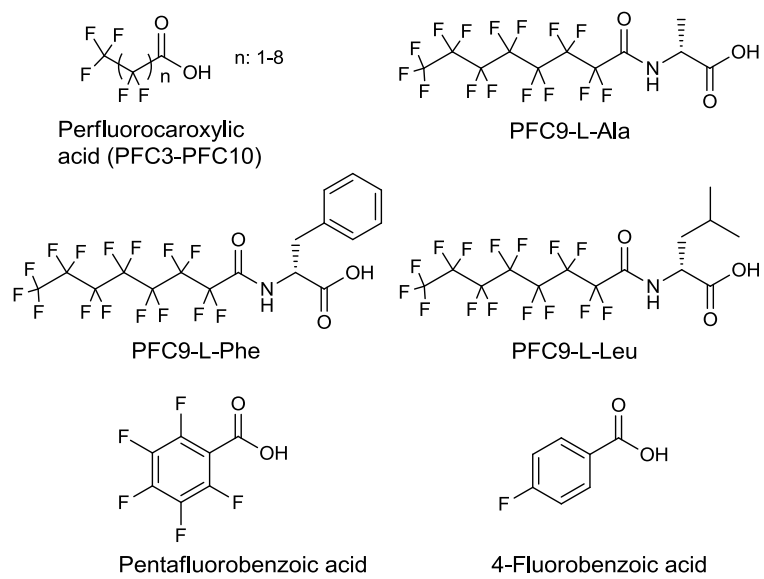


Figure 5 NADPH oxidation (grey) and product formation rates (blue-lined) of turnovers of cyclopentane and cyclohexane with WT, RP and KT2 variants in combination with the second generation of decoy molecules. NADPH oxidation rate and product formation rate are reported as mean ($n \geq 3$) and given in $\text{nmol}(\text{nmol-CYP})^{-1}\text{min}^{-1}$ (full data provided in Table S2).

